

Posttreatment ADC changes in the periresectional area in patients with glioblastoma

Anouk van der Hoorn, MD PhD¹⁻³; Jiun-Lin Yan, MD^{1,4-5}; Timothy J Larkin, PhD¹; Natalie R Boonzaier, MSc¹, Tomasz Matys, MD PhD²; Stephen J Price, PhD FRCS(Neuro Surg.)¹

¹ Brain tumour imaging laboratory, Division of neurosurgery, Department of clinical neuroscience, University of Cambridge, Addenbrooke's hospital, Box 167, CB2 0QQ, Cambridge, United Kingdom;

² Department of radiology, University of Cambridge, Addenbrooke's hospital, Box 218, CB2 0QQ, Cambridge, United Kingdom;

³ Department of radiology (EB44), University Medical Centre Groningen, University of Groningen, Box 30.001, 9700 RB, Groningen, The Netherlands;

⁴ Department of neurosurgery, Chang Gung Memorial Hospital, 204, Keelung, Taiwan

⁵ Department of neurosurgery, Chang Gung University College of Medicine, 333, Taoyuan, Taiwan

Corresponding author:

Anouk van der Hoorn

Department of radiology (EB44)

University Medical Centre Groningen

University of Groningen

Box 30.001, 9700 RB

Groningen

The Netherlands

Phone: +31 50 361 4263

Fax: +31 50 361 1798

Email address: a.van.der.hoorn@umcg.nl

E-mail addresses: a.van.der.hoorn@umcg; jly27@cam.ac.uk; tl347@cam.ac.uk; nrb45@cam.ac.uk; tm418@cam.ac.uk; sjp58@cam.ac.uk

Number of tables: 1

Numbers of figures: 2

Short title: Posttreatment periresectional ADC in GBM

Keywords: ADC; brain tumours; glioblastoma; MRI; treatment response

Abbreviations: ADC=apparent diffusion coefficients; FSL=FMRIB Software Library; MGMT=methylguanin-DNA-methyltransferase; T=Tesla; TE=echo time; TR=repitition time

ABSTRACT

BACKGROUND AND PURPOSE: Although targeted by radiotherapy, recurrence in glioblastoma occurs mainly periresectional due to tumour infiltration. An increase in ADC is shown posttreatment in the large high T2 area, however, until now ADC has not been investigated for the more relevant directly periresectional area.

METHODS: Histogram analysis was used to assess periresectional ADC values in glioblastoma patients postradiotherapy versus preradiotherapy. Periresectional ADC values of 0-5 mm with 5 mm increment up to 20-25 mm were extracted and compared with a two-way repeated measurement ANOVA.

RESULTS: Mean ADC values were significantly higher postradiotherapy directly adjacent to the resection area (0-5 mm) compared to preradiotherapy ($p=0.017$). The 0-5 mm ADC values were also higher than those in 5-10, 10-15 and 15-20 mm regions ($p<0.05$). Regional standard deviations of ADC values were higher postradiotherapy compared to preradiotherapy for the 0-5 up to 15-20 mm region, inclusive ($p<0.05$). Cox regression analysis however showed no survival benefits for the 0-5 mm area increase in ADC postradiotherapy.

CONCLUSIONS: Increased ADC values representing a decrease in infiltrative tumour load was demonstrated in a limited direct periresectional area. This adds to previous studies looking at the larger high T2 area showing ADC response in relation to survival.

INTRODUCTION

Brain tumours are an expanding research area with a significant population burden. Glioblastomas are the most prevalent primary brain tumours, and one of the leading cancers in terms of years of life lost [1]. These tumours tend to recur despite maximal surgical resection of the contrast enhancing region of the tumour. This is followed by radiotherapy targeted at the surroundings of the resection area and combined with temozolomide chemotherapy [2]. Despite this, recurrence is still inevitable, happening even in all patients with a total resection of the contrast enhancing tumour and subsequent chemoradiotherapy. Recurrence occurs within or directly adjacent to the resection area in up to 90% [3], likely due to the infiltrative nature of the tumour spreading beyond the contrast enhancing region [4].

Recent studies demonstrated the potential of apparent diffusion coefficients (ADC) values for evaluating tumour recurrence. In a group of 20 brain tumour patients of which 7 had a glioblastoma, early changes in functional diffusion maps could be used to predict treatment response in patients treated with radiotherapy, chemotherapy or a combination of both [5]. Functional diffusion maps also identified response patterns in patients with glioblastomas treated with boron neutron capture therapy [6]. This was further supported in a rat glioblastoma model showing a correlation between histological decline in tumour cell density and increase in ADC days after the start of chemotherapy [7,8], which also correlated for spatial heterogeneity of ADC response and tumour cell density [8]. Correlation between cell density and ADC has also been demonstrated in patients with untreated glioblastomas [9].

Studies that assess ADC changes after radiotherapy are scarce. Studies in glioblastoma patients, of whom less than 50% received a total resection, showed an increase of ADC values postradiotherapy in comparison with preradiotherapy values in the residual contrast enhancing tumour and in the surrounding T2-hyperintense area [10,11]. This was also related to survival in both studies [10,11].

However, as advanced surgical techniques such as neuronavigation and intraoperative 5-aminolevulinic acid (5-ALA) fluorescence guidance [12] allow resection of more than 90% of the contrast enhancing tumour volume, assessment of ADC values in this contrast enhancing region is of little practical relevance. Similarly, the large area of T2-hyperintense tumour is composed of both infiltrating tumour and vasogenic oedema. It thus can extend far beyond the original contrast enhancement and thus also beyond the periresection area where tumour recurrence is most likely to occur [3].

This prompted us to assess the ADC values specifically in a smaller periresection area using pre- and postradiotherapy MRI scans in patients with a glioblastoma treated with surgical resection and standard concomitant and adjuvant chemoradiotherapy.

METHODS

Patient inclusion criteria

Patients with a newly diagnosed cerebral glioblastoma were included in this study. Patients were collected consecutively from 2010-2014. We included all patients with MRI follow up data from a initial cohort designed for a preoperative imaging study. Exclusion criteria were previous cranial surgery, previous cerebral radiotherapy, a known other primary tumour or follow-up outside our hospitals. Patients with a glioblastoma crossing the midline were not excluded. We included 14 patients (see Table 1 for general characteristics). Tumour location was defined as previously described [13]. All patients were on a stable dexamethasone dose and had a Karnofsky performance status ≥ 70 . Surgical resection was performed using neuronavigation (StealthStation, Medtronic) and 5-ALA fluorescence guidance with the aim of maximal resection. Surgery was followed by standard concomitant chemoradiotherapy and adjuvant chemotherapy [2] starting 4 weeks after surgery. Radiotherapy consisted of 60 Gy following the EORTC protocol with 60Gy in 30 fractions (2Gy

fractions given once daily for five days a week over a six week period) [14]. Radiotherapy was delivered to the resection margin with a total margin of 3 cm in all patients. Follow-up MRI scans were collected directly after surgery, as well as pre- and postradiotherapy. The postoperative MRI was performed <72 hours after the operation. Direct preradiotherapy MRI was on average 21 days after the operation (range 14-32), while postradiotherapy MRI was on average 87 days (2.9 months) thereafter (range 77-96 days; 2.6-3.2 months). As preradiotherapy scans were missing in 3 patients, data concerning this time point was based on 11 patients, while other analyses were done on all 14 patients. Progression free survival and overall survival data were established based on medical records. Progression free survival was defined according to the RANO criteria [15].

The study was approved by the local Institutional Review Board and informed written consent was obtained from all patients.

Data acquisition

MRI scans were acquired on a 1.5 T GE Optima, 1.5 or 3.0 T GE Signa or 3.0 T GE Discovery (General Electric Company, Little Chalfont, United Kingdom) with a standard head coil. Imaging included a T1-weighted anatomical sequence after the intravenous injection of 9 ml gadolinium (Gadovist, Bayer Schering Pharma, Berlin, Germany). This was performed as a 2D T1-weighted sequence (TR/TE 400-784/11-20 ms, flip angle 90-160°, FOV 220-240 x 220-240 mm; 20-84 slices; 0-1 mm slice gap; voxel size 0.43-0.86 x 0.43-0.86 x 2-6 mm) or a 2D T1 inversion recovery sequence (TR/TE 2508-2590/12-42 ms, inversion time 780-920 ms; flip angle 90-110°, FOV 220 x 220 mm; 20-22 slices; 1-3.5 mm slice gap; voxel size of 0.43 x 0.43 x 6 mm).

DWI data was acquired using a single-shot echo-planar sequence (TR/TE 6000-12500/64-108 ms; flip angle 90°; FOV 220-300 x 220-300 mm; 52-66 slices; 0-4 mm slice gap; voxel size 0.86-1.2 x 0.86-1.2 x 4-5 mm) using a b-value of 0 and 1000 s/mm² scanned in 3-25 directions.

ADC analysis

ADC images were coregistered to the T1-weighted post contrast images of the same time point using tools from the FMRIB Software Library (FSL) version 5.0.0 (www.fmrib.ox.ac.uk/fsl). The brain images were automatically extracted [16] and manually corrected. A linear transformation of the brain images was done using the FLIRT function, resulting in ADC images coregistered to post contrast T1 images.

ADC data were normalised to the contralateral normal appearing white matter. Contralateral MRI abnormality in for instance a glioblastoma crossing the midline were avoided in this process. The resection cavity was identified with an automatic segmentation using the FSL FAST function [17] and manually corrected. The resection cavity was dilated to create a 3D region of 0-5, 5-10, 10-15, 15-20 and 20-25 mm around the resection (Figure 1) as these are the most common areas for tumour recurrence [3,18] and thus most relevant for treatment evaluation using ADC values. The resection cavity itself, ventricles and areas outside of the brain were excluded.

Statistical analysis

In general, direct postoperative ADC values were similar to direct preradiotherapy. We therefore used preradiotherapy ADC values as primary baseline for comparison to postradiotherapy images. In addition, we compared the direct postoperative images with the postradiotherapy images as a preradiotherapy ADC is not acquired as standard in all clinical practices. Histogram analysis was used testing the mean, standard deviation, skewness and kurtosis. Skewness indicates the asymmetry of the distribution, while kurtosis represents the width and height of a distribution. Both represent the heterogeneity of a distribution, but in a different way, meaning that both can be normal or abnormal independent from each other. A two-way within subject analysis of variance was conducted to assess ADC values at different distances from the resection cavity using five factors starting with 0-5 mm from the resection cavity with 5 mm increments up to 20-25 mm from the resection cavity. Two time

points were entered as factor (before and after radiotherapy). A similar analysis of variance was conducted for directly postoperative versus postradiotherapy. Mauchly's test of sphericity was used to test the sphericity for the main effect of distance and interaction between time and distance. As the assumption of sphericity was violated in all cases, we used Greenhouse-Geisser corrected output for all analyses of variance. Post-hoc comparisons used a paired t-test or Wilcoxon-signed rank test depending on the normality. The normality was tested using the Shapiro-Wilk test.

We further investigated the predictive value of the increase of the postradiotherapy ADC of the 0-5 mm area for the progression free survival and overall survival, first using a univariate Cox regression model. Secondly, a multivariate Cox regression model was used correcting for age and O⁶-methylguanin-DNA-methyltransferase (MGMT) methylation status. The Cox proportional hazard assumption test were performed for all Cox regression models showing no violation of this assumption.

Two-sided *p*-values were used throughout. All statistical tests were performed using SPSS version 22 (IBM Inc., New York, USA).

RESULTS

Histogram analysis

Group mean, standard deviations, skewness and kurtosis of the patients mean of the periresection voxels are demonstrated (Figure 2).

Mean ADC values at different distances from the resection cavity showed a significant interaction between time and distance (Figure 2A) ($F(1.8,18)=5.4, p=0.018$). There was no significant main effect of time ($F(1,10)=1.9, p=0.195$) or distance ($F(1.2,12)=2.5, p=0.062$). Post-hoc comparison showed a statistically significant increase in the ADC value directly adjacent (0-5 mm) to the resection cavity postradiotherapy in comparison to preradiotherapy ($t(10)=-2.8, p=0.017$). Postoperative values increased 0.19, from 1.29 to 1.48. Furthermore, for the postradiotherapy data, the 0-5 mm region

differed significantly from the 5-10 ($t(13)=2.8, p=0.014$), 10-15 ($t(13)=3.0, p=0.010$), 15-20 ($t(13)=3.2, p=0.007$) and 20-25 mm region ($t(13)=3.3, p=0.006$). The 5-10 mm region also was significantly different to the 20-25 mm region ($t(13)=2.3, p=0.038$).

The mean postoperative ADC values compared to postradiotherapy showed no significant interaction between time and distance ($F(1.4,18)=2.1, p=0.158$). There was no main effect of time ($F(1,13)=1.1, p=0.311$), but there was for distance ($F(1.3,16)=5.6, p=0.024$). Post-hoc comparison only revealed a marginally statistical significant result for the 0-5 mm region ($t(13)=-2.1, p=0.051$).

To demonstrate the heterogeneity of the voxels within the region of interest the standard deviations were compared (Figure 2B). There was no significant interaction between time and distance ($F(1.5,15)=0.95, p=0.384$) comparing postradiotherapy with preradiotherapy. There was a significant main effect of time ($F(1,10)=13.5, p=0.004$). There was no main effect of distance ($F(1.5,15)=0.52, p=0.556$). Post-hoc comparison for the time showed a statistically significant difference for the 0-5 mm region, which demonstrated a higher standard deviation postradiotherapy compared to preradiotherapy ($Z=2.1, p=0.033$). The same was true comparing the postradiotherapy with the preradiotherapy for the 5-10 ($t(10)=-3.1, p=0.011$), 10-15 ($t(13)=-4.3, p=0.002$) and 15-20 mm region ($t(13)=-3.2, p=0.010$), but it was only marginally significant for the 20-25 mm region ($t(13)=-2.2, p=0.051$).

Postoperative compared to postradiotherapy standard deviations showed no significant interaction between time and distance ($F(1.5,19.9)=0.64, p=0.499$). There was a significant main effect of time ($F(1,13)=5.6, p=0.034$), but not for distance ($F(1.2,16)=0.88, p=0.386$). Post-hoc comparison for the time showed that the 5-10 mm region was higher postradiotherapy than postoperative ($Z=2.3, p=0.022$). Other regions demonstrated no statistically significant differences.

Analysis of skewness (Figure 2C) representing the asymmetry of the histogram demonstrated no significant interaction comparing postradiotherapy with preradiotherapy ($F(2.1,21)=0.93, p=0.414$).

No significant main effect of time was demonstrated ($F(1,10)=2.5, p=0.148$). A significant main effect of distance was present ($F(1.3,13)=9.7, p=0.006$). Post-hoc testing showed a significantly lower skewness for the 0-5 mm region in comparison to the 5-10 ($t(13)=-2.3, p=0.037$), 10-15 ($t(13)=-3.9, p=0.002$), 15-20 ($t(13)=-4.1, p=0.001$) and 20-25 mm region ($t(13)=-4.1, p=0.001$) in the postradiotherapy data. The 5-10 mm region was also significantly lower compared to the 10-15 ($t()=-2.5, p=0.027$), 15-20 ($t()=-2.8, p=0.015$) and 20-25 mm region ($t()=-2.4, p=0.034$) postradiotherapy. There were no significant differences within the preradiotherapy time point although values were similar, but slightly less different than postradiotherapy.

Comparing the skewness of the postoperative with the postradiotherapy images showed similar results. There was no significant interaction between distance and time ($F(2.5,33)=2.4, p=0.093$) or main effect for time ($F(1,13)=0.11, p=0.750$). A significant main effect was found for distance ($F(2.1,27)=8.9, p<0.001$). Post-hoc tests of postradiotherapy results are already described. Postoperative values were comparable, but there was only a statistically significant difference for the 0-5 mm region in comparison to the 20-25 mm region ($t()=-2.3, p=0.038$).

Kurtosis analysis (Figure 2D) indicating the height and sharpness of the histogram for the postradiotherapy and preradiotherapy time point showed no significant interaction ($F(1.5,15)=0.084, p=0.869$) and no main effect of time ($F(1,10)=3.2, p=0.106$). A significant main effect was shown for distance ($F(1.7,17)=4.8, p=0.026$). Post-hoc testing within the postradiotherapy data revealed a flatter and wider distribution for the 0-5 mm region compared to the 10-15 ($t(13)=-2.6, p=0.021$), 15-20 ($t(13)=-3.0, p=0.011$) and 20-25 mm region ($t(13)=-2.9, p=0.013$). The 5-10 mm region was also lower than the 10-15 ($t(13)=-2.9, p=0.011$), 15-20 ($t(13)=-3.1, p=0.008$) and 20-25 mm region ($t(13)=-3.3, p=0.006$). A similar distribution was seen preradiotherapy, but without statistically significant differences.

Kurtosis of postoperative compared to postradiotherapy showed no interaction between time and distance ($F(1.8,23)=0.39, p=0.657$). No main effect for time was demonstrated ($F(1,13)=0.66,$

$p=0.430$). A significant main effect for distance was shown ($F(2.6, 34)=11.4, p<0.001$). The postoperative distribution resembled the preradiotherapy and postradiotherapy distribution. Post-hoc testing within the postoperative moment demonstrated a statistically significant lower kurtosis for the 0-5 mm region in comparison to the 5-10 ($Z=2.2, p=0.026$), 10-15 ($Z=2.5, p=0.011$), 15-20 ($Z=2.5, p=0.011$) and 20-25 mm region ($Z=2.4, p=0.016$).

Survival analysis

The increase in ADC value postradiotherapy in comparison to preradiotherapy for the 0-5 mm area did not predict an increase in progression free survival ($HR=0.414, p=0.711$) or overall survival ($HR=0.224, p=0.692$). This did not change significantly after adjusting for age and MGMT status with a multivariate Cox regression model.

DISCUSSION

This is the first study to selectively analyse periresectional change of ADC values, as previous research has only looked at the large high T2 area [10,11]. We demonstrated that mean ADC values were most likely to increase in the area directly adjacent to the resection cavity (0-5 mm), while moving further away, the changes quickly became less pronounced. The highest infiltrating tumour load is also to be expected in the 0-5 mm area. The demonstrated heterogeneity of the skewness and kurtosis postradiotherapy might possible be also explained by this higher a priori tumour load as well as heterogeneity in tumour response most pronounced in this area were most tumour is present.

Although a histological correlation has not been performed in this study, previous research has validated the correlation between ADC values and viable tumour cells in rats [7,9] and humans [9] with glioblastoma. Furthermore, ADC changes preceded contrast enhancement in tumour recurrence indicating the recurrence of tumour cells before these cells induce a disruption of the blood-brain

barrier [19]. Observed increase in ADC values after treatment therefore indicate a reduction of tumour cellularity due to radiotherapy.

Reduction of tumour cell density in the direct peritumoural area is of specific interest. Radiotherapy currently targets the resection site and the adjacent region, which was also the case for the patients in our study in combination with chemotherapy. However, this is insufficient as recurrence is still inevitable and occurs in about 90% of the patients within or directly adjacent to the resection area [3]. Low ADC indicative of a high amount of tumour cells in recurrent glioblastoma seen in 95% within the 60 Gy isodose line is associated with poorer outcome [20]. This might be due to the variable treatment response of glioblastoma cells [8], which is also suggested by our increased standard deviation postradiotherapy. Even more focus on localised therapy thus seems logical and therapy like Carmustine wafers is of interest [21]. In these cases, however, one would expect to see a survival benefit in patients with ADC response, which we were unable to demonstrate. Our absent correlation with survival might be due to the small group size and could also be partially influenced by treatment given after finishing chemoradiotherapy and tumour progression. However, others have clearly demonstrated a correlation between an increase in ADC values after treatment and outcome. Studies in glioblastoma patients with mixed nonsurgical treatment showed that ADC in the high T2 region differs in patients with progression of the T2 and patients with stable T2 disease [22]. The same holds for the contrast enhancing area [10,23] and FLAIR area [10]. However, others demonstrate no correlation with ADC values after treatment but instead demonstrated a correlation of midtreatment ADC values with survival [24]. The correlation with survival is demonstrated for preradiotherapy ADC values in the FLAIR region correlating with progression free survival and overall survival in patients with glioblastoma, most of them with a subtotal resection [25]. Preradiotherapy ADC values also might be more accurate than direct postoperative values due to minor areas with lower ADC values directly postoperative caused by minor ischemic changes. As our ADC postoperative is slightly higher in the 0-5 mm area in comparison to preradiotherapy ischemic

changes is unlikely to have influenced postoperative values. Ischemic changes would not be a confounding factor in the preradiotherapy scans as they were all acquired >14 days (mean 21 days) after the operation, at which time any restricted diffusion secondary to ischaemic changes would normalise.

One of the main future applications of ADC response would be the early stratification of patients into responders and nonresponders. This would provide more time for secondary therapeutic interventions, which increases their chance of being effective. It also could prevent unnecessary ineffective, possible toxic and costly treatment in non-responders. Anatomical MRI using the increase in tumour size is incapable of demonstrating early changes. As a result, research has focussed on apparent diffusion coefficients calculated from diffusion weighted MRI. We are the first to show the increase of ADC specific to the area adjacent to the resection as result of chemoradiotherapy after the end of radiotherapy. Others have shown that ADC is also capable of demonstrating an early change in a population with mixed brain tumour [5] and in a rat model with glioblastoma [7,8]. ADC is thus a potential early imaging biomarker of treatment response. Further research should focus on periresectional ADC values in glioblastoma patients early in the current standard treatment, but also in studies investigating new localised therapies.

In such research, voxel-based ADC response parameters are likely to be more accurate than a single posttreatment measurement and parametric response maps have been shown to outperform a single posttreatment measurement for the prediction of outcome at 3 months and 1 year in treated glioblastoma patients [26]. A parametric response map, however, needs 3D volumetric acquisitions pre- and posttreatment. This is often not acquired as standard in clinical practice. Our more simplified histogram calculations using 2D MRI data therefore has wider applicability. We also used MRI scanners of different manufactures and field strengths. To overcome the known variation that can result from this [27], we successfully used ADC values normalised to the contralateral normal

appearing white matter. This is also an advantage for the applicability of histogram ADC response calculations in clinical practice, in which one also have to deal with different MRI scanners and different ADC settings with most commonly used 2D acquisitions.

Nevertheless, voxel-based ADC analysis in glioblastoma patients are in line with our histogram results, although previous studies have not looked specifically at the periresection area. A comparable patient population of which most also received surgery showed higher ADC values posttreatment [24]. Others have shown similar results in patients without surgery treated with radiotherapy or chemotherapy [5] and boron neutron capture therapy [6] at the location of the primary tumour. An increase of ADC values postradiotherapy in comparison with preradiotherapy values in the contrast enhancing tumour and in the area with high T2 signal was also been demonstrated [10,11].

A few limitation can be identified in our study. The relatively small sample size and absence of a correlation with survival in our study has been discussed above. Another limitation is the lack of histological confirmation. However, a higher viable tumour load has been confirmed to correspond with lower ADC values in glioblastoma patients previously [9] making that we can interpret our ADC values as representing tumour load as also describe in the second paragraph of the discussion.

CONCLUSIONS

In conclusion, we calculate ADC response in the periresection area and showed an increase in ADC postradiotherapy. This has not been demonstrated previously in the periresectional region, but is in line with studies looking at the large areas with high T2 showing a higher ADC posttreatment in correlation with a better outcome.

CONFLICT OF INTEREST

All authors declare that they have no conflict of interest.

REFERENCES

- 1 Burnet NG, Jefferies SJ, Benson RJ, Hunt DP, Treasure FP (2005) Years of life lost (YLL) from cancer is an important measure of population burden and should be considered when allocating research funds. *J Cancer* 92:241-245.
- 2 Stupp R, Mason WP, van den Bent MJ et al. (2005) Radiotherapy plus concomitant and adjuvant temozolomide for glioblastoma. *NEJM* 352:987-996.
- 3 Petrecca K, Guiot MC, Panet-Raymond V, Souhami L (2013) Failure pattern following complete resection plus radiotherapy and temozolomide is at the resection margin in patients with glioblastoma. *J Neurooncol* 111:19-23.
- 4 Lemée JM, Clavreul A, Menei P (2015) Intratumoral heterogeneity in glioblastoma: don't forget the peritumoral brain zone. *Neuro Oncol* 17:1322-1332.
- 5 Moffat BA, Chenevert TL, Lawrence TS, et al. (2005) Functional diffusion map: A noninvasive MRI biomarker for early stratification of clinical brain tumor response. *PNAS* 102:5524-5529.
- 6 Hiramatsu R, Kawabata S, Furuse M, Miyatake SI, Kuroiwa T (2013) Identification of early and distinct glioblastoma response patterns treated by boron neutron capture therapy not predicted by standard radiographic assessment using functional diffusion map. *Radiat Oncol* 8:192.
- 7 Chenevert TL, Stegman LD, Taylor JMG et al. (2010) Diffusion magnetic resonance imaging: an early surrogate marker of therapeutic efficacy in brain tumors. *J Natl Cancer Inst* 92:2029-2036.
- 8 Moffat BA, Chenevert TL, Meyer CR, Mckeever PE, Haal DE, Hoff BA, Johnson TD, Rehemtulla A, Ross BD (2006) The functional diffusion map: An imaging biomarker for the early prediction of cancer treatment outcome. *Neoplasia* 8:259-267.

- 9 Ellingson BM, Malkin MG, Rand SD et al. (2010) Validation of functional diffusion maps (fDMs) as a biomarker for human gliomas cellularity. *J Magn Reson Imaging* 31:538-548.
- 10 Ellingson BM, Cloughesy TF, Zaw T et al. (2012) Functional diffusion maps (fDMs) evaluated before and after radiochemotherapy predict progression-free and overall survival in newly diagnosed glioblastoma. *Neuro Oncol* 14:333-343.
- 11 Li Y, Lupo JM, Polley MY, Crane JC et al. (2011) Serial analysis of imaging parameters in patients with newly diagnosed glioblastoma multiforme. *Neuro Oncol* 13:546-557.
- 12 Valle RD, Solis ST, Gastearna MAI, de Eulate RG, Echávarri PD, Mendiroz JA (2011) Surgery guided by 5-aminolevulinic fluorescence in glioblastoma: Volumetric analysis of extent of resection in single-center experience. *J Neurooncol* 102:105-113.
- 13 Sawaya RE, Hammound M, Schoppa D et al. (1998) Neurosurgical outcomes in a modern series of 400 craniotomies for treatment of parenchymal tumors. *Neurosurgery* 42:1044-1055.
- 14 Stupp R, Hegi ME, Mason WP et al. (2009) Effects of radiotherapy with concomitant and adjuvant temozolomide versus radiotherapy alone on survival in glioblastoma in a randomised phase III study: 5-year analysis of the EORTC-NCIC trial. *Lancet Oncol* 10:459-466.
- 15 Wen PY, Macdonald DR, Reardon DA et al. (2010) Updated response assessment criteria for high-grade gliomas: response assessment in neuro-oncology working group. *J Clin Oncol* 28:1963-1972.
- 16 Smith SM (2002) Fast robust automated brain extraction. *Hum Brain Mapp* 17:143-155.
- 17 Zhang Y, Brady M, Smith S (2001) Segmentation of brain MR images through a hidden markov random field model and the expectation-maximization algorithm. *IEEE T Med Imaging* 20:45-57.
- 18 De Bonis P, Anile C, Pompucci A et al. (2013) The influence of surgery on recurrence pattern of glioblastoma. *Clin Neurol Neurosurg* 115:37-43.
- 19 Gupta A, Young RJ, Karimi S et al. (2011) Isolated diffusion restriction precedes the development of enhancing tumor in a subset of patients with glioblastoma. *AJNR Am J Neuroradiol* 32:1301-1306.

- 20 Elson A, Paulson E, Bovi J, Siker M, Schultz C, Laviolette PS (2015) Evaluation of pre-radiotherapy apparent diffusion coefficient (ADC): patterns of recurrence and survival outcomes analysis in patients treated for glioblastoma multiforme. *J Neurooncol* 123:179-188.
- 21 Xing WK, Shao C, Qi ZY, Yang C, Wang Z (2015) The role of Gliadel wafers in the treatment of newly diagnosed GBM: a meta-analysis. *Drug Des Devel Ther* 9:3341-3348
- 22 Lutz K, Wiestler B, Graf M et al. (2014) Infiltrative patterns of glioblastoma: Identification of tumor progress using apparent diffusion coefficient histograms. *J Magn Reson Imaging* 39:1096-1103.
- 23 Chang W, Pope WB, Harris RJ et al. (2015) Diffusion MR Characteristics Following Concurrent Radiochemotherapy Predicts Progression-Free and Overall Survival in Newly Diagnosed Glioblastoma. *Tomography* 1:37-43.
- 24 Khayal IS, Polley MY, Jalbert L et al. (2010) Evaluation of diffusion parameters as early biomarkers of disease progression in glioblastoma multiforme. *Neuro Oncol* 12:908-16.
- 25 Elson A, Bovi J, Siker M, Schultz C, Paulson E (2015) Evaluation of absolute and normalized apparent diffusion coefficients (ADC) values within the post-operative T2/FLAIR volume as adverse prognostic indicators in glioblastoma. *J Neurooncol* 122:549-558.
- 26 Yoon RG, Kim HS, Kim DY, Hong GS, Kim SJ (2015) Apparent diffusion coefficient parametric response mapping MRI for follow-up of glioblastoma. *Eur Radiol* in press (DOI 10.1007/s00330-015-3896-8).
- 27 Sasaki M, Yamada K, Watanabe Y et al. (2008) Variability in absolute apparent diffusion coefficient values across different platforms may be substantial: A multivendor, multi-institutional comparison study. *Radiology* 249:624-630.

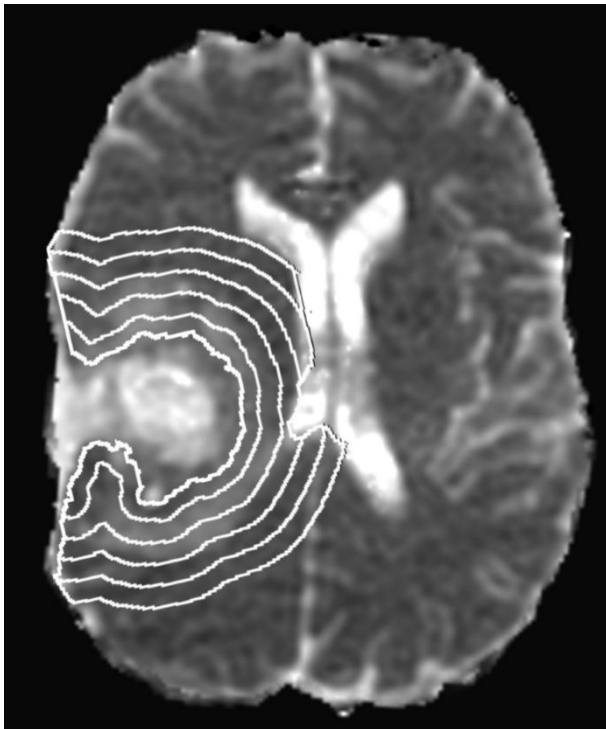
TABLE 1 - Patient Characteristics

Total number of patients	14
Male	7
Female	7
Age (years)	57 (11)
Tumour location	
Eloquent	5
Near eloquent	4
Non eloquent	5
Midline shift (mm)	3.8 (3.9)
Preoperative tumour size (ml)	
T1 contrast enhanced	40 (29)
FLAIR	88 (50)
Resection cavity (ml)	
Postoperative	35 (39)
Preradiotherapy	46 (39)
Postradiotherapy	22 (33)
GTR (based on contrast)	9
STR (based on contrast)	5
Progression Free Survival (days)	295 (209)
Overall Survival (days)	515 (273)
MGMT status	
Negative	6
Positive	2
Unknown	6
IDH-1 mutation	
Negative	14
Positive	0
Unknown	0

Numbers or mean values and standard deviations are presented for the main patient characteristics.

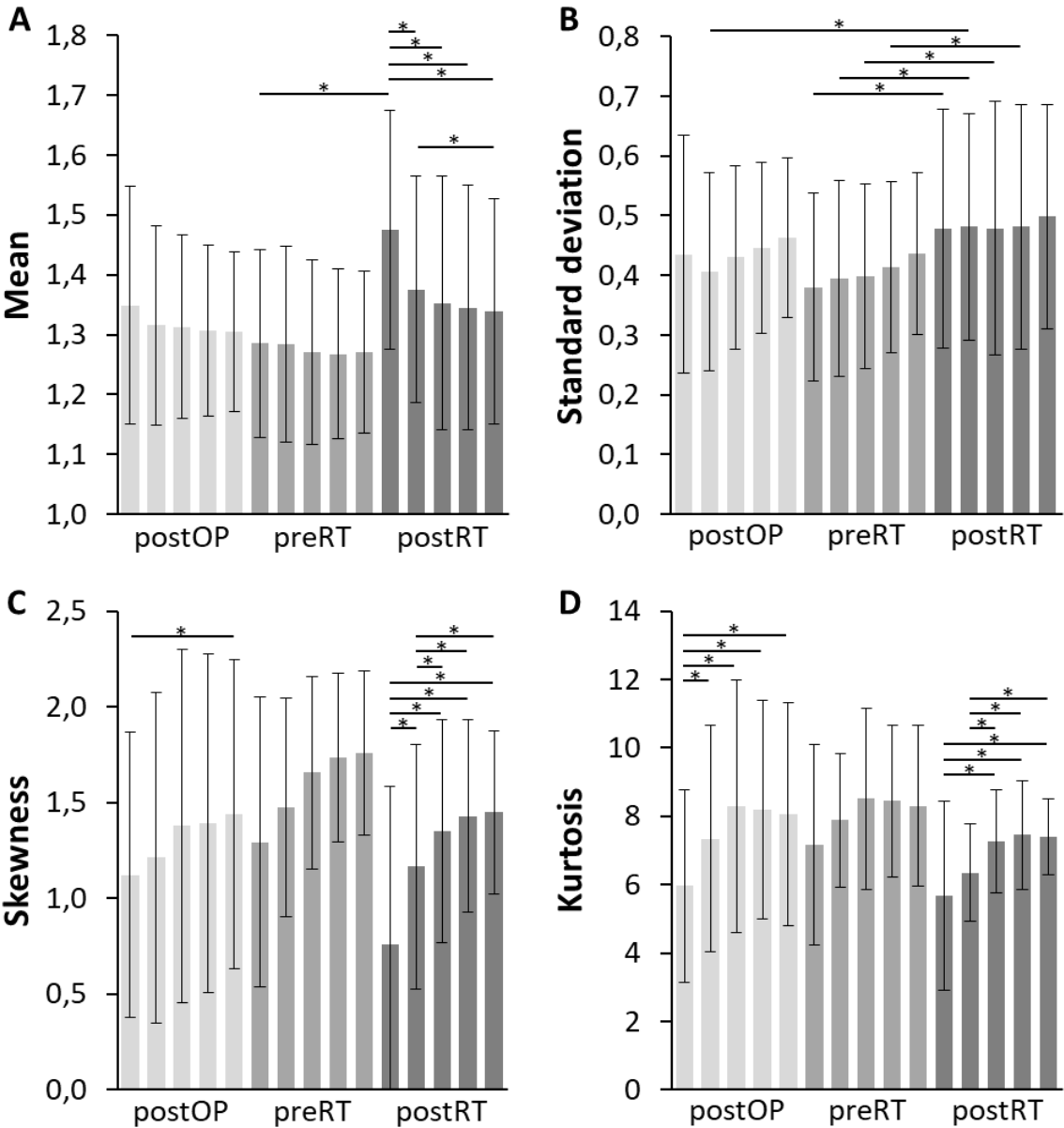
Abbreviations: GTR=gross total resection; IDH=isocitrate dehydrogenase; MGMT=O6-methylguanine-DNA-methyltransferase; ml=millilitre; mm=millimetre; STR=subtotal resection.

FIGURE 1 – Periresectional regions on ADC



Periresectional regions of interest are displayed for the preradiotherapy ADC map of a representative patients. Regions are 0-5 mm with 5 mm increments to 20-25, inclusive.

FIGURE 2 – Normalised ADC in the periresection areas



Histogram analysis of normalised apparent diffusion coefficient (ADC) values are displayed. The periresectional area of the postOP, preRT and postRT is divided in 5 regions starting from 0-5 mm periresectional with 5 mm increment up to 20-25 mm. Group means and standard deviation are shown for the subjects mean (A), standard deviation (B), skewness (C) and kurtosis (D). Significant post-hoc tests ($p < 0.05$) are displayed if the main effect or interaction was significant (*). Abbreviations: postOP=postoperative; preRT=preradiotherapy; postRT=postradiotherapy.